A study of the interaction between cucurbit[8]uril and alkyl substituted 4-pyrrolidinopyridinium salts

Weitao Xu,[a] Jinglan Kan,[b] Bo Yang,[a] Timothy J. Prior,[c] Bing Bian,[d] Xin Xiao,[a*] Zhu Tao,[a] and Carl Redshaw[c*]

[a] *State Key Laboratory Breeding Base of Green Pesticide and Agricultural Bioengineering, Key Laboratory of Green Pesticide and Agricultural Bioengineering, Key Laboratory of Macrocyclic and Supramolecular Chemistry of Guizhou Province, Guizhou University, Guiyang 550025, China*

[b] *College of Chemistry, Chemical Engineering and Materials Science, Collaborative Innovation Center of Functionalized Probes for Chemical Imaging in Universities of Shandong, Key Laboratory of Molecular and Nano Probes, Ministry of Education, Shandong Normal University, Jinan 250014, P. R. China.*

[c] *Chemistry, School of Mathematics and Physical Sciences, University of Hull, Hull HU6 7RX, U.K.*

[d] *College of Chemistry and Environmental Engineering, Shandong University of Science and Technology, Qingdao 266590, China.*

Abstract: The interaction between cucuribit[8]uril (Q[8]) and a series of 4-pyrrolidinopyridinium salts bearing aliphatic substituents at the pyridinium nitrogen, namely 4-$(C_4H_8N)C_5H_5NRBr$, where R = Et (g1), *n*-butyl (g2), *n*-pentyl (g3), *n*-hexyl (g4), *n*-octyl (g5), *n*-dodecyl (g6), has been studied in aqueous solution by ^{1}H NMR spectroscopy,

electronic absorption spectroscopy, Isothermal Titration Calorimetry and mass spectrometry. Single crystal X-ray diffraction revealed the structure of the host-guest complexes for g1, g2, g3, and g5. In each case the Q[8] contains two guest molecules in a centrosymmetric dimer. The orientation of the guest molecule changes as the alkyl chain increases in length. Interestingly, in the solid state, the inclusion complexes identified are different from those observed in solution, and furthermore, in the case of g3, Q[8] exhibits two different interactions with the guest. In solution, the length of the alkyl chain plays a significant role in determining the type of host-guest interaction present.

Introduction

Molecular recognition by cucurbit[n]uril (Q[n]) systems has flourished in recent years. [1] A variety of guests have been studied, primarily for Q[6 to 8], with encapsulation in the hydrophobic cavity often observed. [2] Among them, the host-guest behaviour of Q[n]s towards a variety of organic cations including ammonium ions, viologens as well as pyridinium salts, with high binding constants has been reported. [3] Our group has also investigated the binding interaction of Q[n]s with a series of pyridinium salts. [4] In particular, we have investigated the nature of the of the host-guest complex between Q[6] and *N*-butyl-4-pyrrolidinopyridine (BuPC4). In this example, only the butyl chain of the guest was found to reside in the cavity, [5] this despite the presence of other active sites such as the pyridyl and tetrahydropyrrole moieties. Given that 4-pyrrolidinopyridines are an important class of *N*-

heteroaromatic compounds that have seen widespread use as catalysts in acyl transfer reactions, [6] we wondered whether the recognition behavior of Q[6] towards BuPC4 was typical for Q[n]s.

Moreover, the presence of alkyl chains can play an important role in biological membranes, liquid crystals, polymers, and functional compounds, as well as in the construction of supramolecular assemblies. Indeed, the length of an alkyl chain can influence molecular recognition processes, the conformations of host-guest species and the switching of functionalities in supramolecular assemblies. [7] One prominent example from the Rebek group is the templation of the alkyl chains of amphiphiles into helical conformations upon binding to a water-soluble cavitand. [8] Kim and co-workers have revealed that the alkyl chains of amphiphiles and bolaamphiphiles respectively adopt 'J-shaped' and 'U-shaped' conformations when bound within the hydrophobic cavity of Q[8]. [9] Contorted conformations of 1,4-butylidenedipyridinium and 1,10-decylidenedipyridinium cationic guests were also studied with a cucurbit[8]uril host by our group. [10] We now extend our host-guest studies to the Q[8] system, and report our observations on its interaction with a series of 4-pyrrolidinopyridinium salts bearing differing lengths of aliphatic substituents at the pyridinium nitrogen, namely 4-(C_4H_8N)C_5H_5NRBr, where R = Et (g1), n-butyl (g2), n-pentyl (g3), n-hexyl (g4), n-octyl (g5), n-dodecyl (g6) (see chart 1).

g1 R=CH_2CH_3 g2 R=$(CH_2)_3CH_3$ g3 R=$(CH_2)_4CH_3$
g4 R=$(CH_2)_5CH_3$ g5 R=$(CH_2)_7CH_3$ g6 R=$(CH_2)_{11}CH_3$
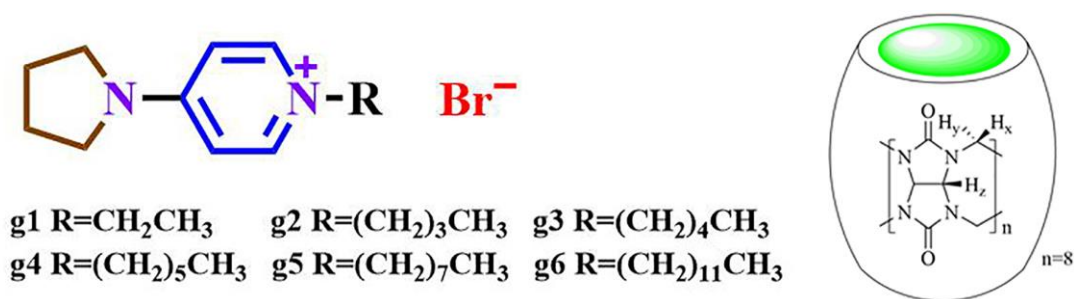
Chart 1. Guests and Q[8] used in this study.

Results and Discussion

NMR spectroscopy

The binding interactions between each of the pyrrolidinopyridinium guests and Q[8] can be conveniently monitored using ^{1}H NMR spectroscopic data recorded in neutral D_2O solution.

In the case of g1:

Figure 1 shows the changes observed in the ^{1}H NMR spectrum of g1 as progressively larger amounts of Q[8] are added to the solution. A slight down-field shift of the signals of the protons of ethyl chain and a clear up-field shift of the signals of the protons of the pyridine and pyrrole rings was observed as Q[8] was added. At 0.87 equiv. of Q[8], the resonances of protons H_d, H_c, H_b and H_a of g1, exhibited an up-field shift of 0.10 ppm (from 7.78 ppm to 7.68 ppm), 0.62 ppm (from 6.53 ppm to 5.91 ppm), 0.70 ppm (from 3.29 ppm to 2.59 ppm) and 0.54 ppm (from 1.86 ppm to 1.32 ppm). By contrast, the protons H_e and H_f of g1 experienced a down-field shift of 0.11 ppm and 0.10 ppm, respectively. At 1.27 equiv. of

Q[8], the resonances of H_d, and H_c of the pyridine of g1, exhibited an up-field shift of 0.09 ppm (from 7.68 ppm to 7.59 ppm) and 0.13 ppm (from 5.91 ppm to 5.78 ppm) respectively, whilst the protons H_e and H_f of ethyl chain of g1 showed essentially no change. The resonances for H_b and H_a of the pyrrole of g1, underwent a down-field shift of 0.04 ppm (from 2.59 ppm to 2.63 ppm) and 0.09 ppm (from 1.32 ppm to 1.41 ppm) respectively compared to the positions at 0.87 equiv. of Q[8]. This indicates that the pyridine and pyrrole rings were accommodated within the cavity of Q[8] and the alkyl chain was out the portal.
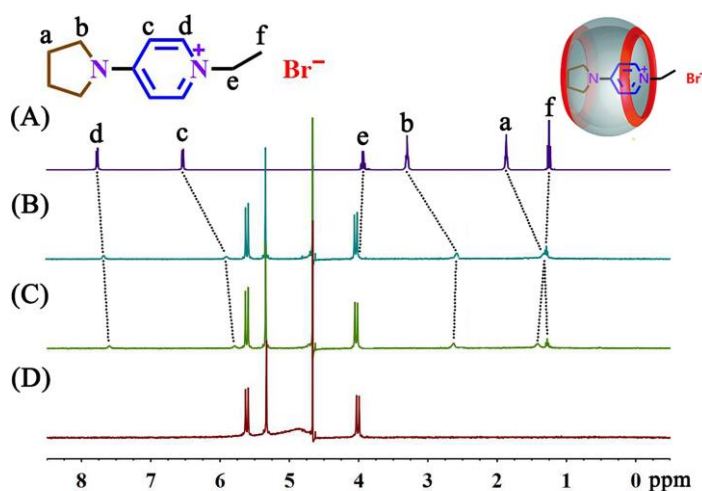

Figure 1. Interaction of g1 and Q[8] (20 °C): ^{1}H NMR spectra (400 MHz, D$_2$O) of g1 (ca. 2 mM) in the absence of Q[8] (A), in the presence of 0.87 equiv. of Q[8] (B), in the presence of 1.27 equiv. of Q[8] (C), and with neat Q[8] (D).

In the case of g2 and g3,

Figure 2 shows the ^{1}H NMR titration spectra of g2 in D_2O recorded in the absence of Q[8] and with increasing proportions of Q[8], and neat Q[8] in D_2O at 20 ℃. Noticeably up-field shifts were observed for all the protons of the pyridine ring, pyrrole ring and alkyl chain as Q[8] was added. At 0.81 equiv. of Q[8], H_d, H_c, H_e, H_b, H_a, H_f, H_g and H_h of g2, exhibited up-field shifts range from 0.09 to 0.44 ppm compared to their positions in free g2. Note that the resonance for H_a was identical to that of H_f. At 1.56 equiv. of Q[8], H_d, H_c, H_e, H_f, H_g and H_h of g1 exhibited up-field shifts of 0.36 ppm (from 7.58 ppm to 7.22 ppm), 0.16 ppm (from 6.14 ppm to 5.98 ppm), 0.12 ppm (from 3.84 ppm to 3.72 ppm), 0.06 ppm (from 1.43 ppm to 1.37 ppm), 0.17 ppm (from 0.96 ppm to 0.79 ppm), 0.24 ppm (from 0.55 ppm to 0.31 ppm), respectively. The protons H_b and H_a of the pyrrole ring of g2 experienced a down-field shift of 0.14 ppm (from 2.90 ppm to 3.04 ppm), 0.19 ppm (from 1.50 ppm to 1.69 ppm), respectively compared to their positions at 0.81 equiv. of Q[8]. Also at this concentration of Q[8], H_a and H_b of the pyrrole of g1, underwent up-field shifts of 0.30 ppm (from 3.34 ppm to 3.04 ppm) and 0.21 ppm (from 1.90 ppm to 1.69 ppm) respectively compared to their positions in free g2. This indicates that the pyridine ring, the pyrrole ring and the alkyl chain are all accommodated within the cavity of Q[8], and that the Q[8] can shuttle on the guest g2 in a state of dynamic equilibrium.

The changes observed in the chemical shifts for all protons of g3 is similar to g2 as Q[8] was added. As shown in Figure S1, obvious up-field shifts for all protons of the pyridine ring, the pyrrole ring and the alkyl chain were observed as the Q[8] was added, which indicates the situation is as for g2, i.e. a state of dynamic equilibrium.
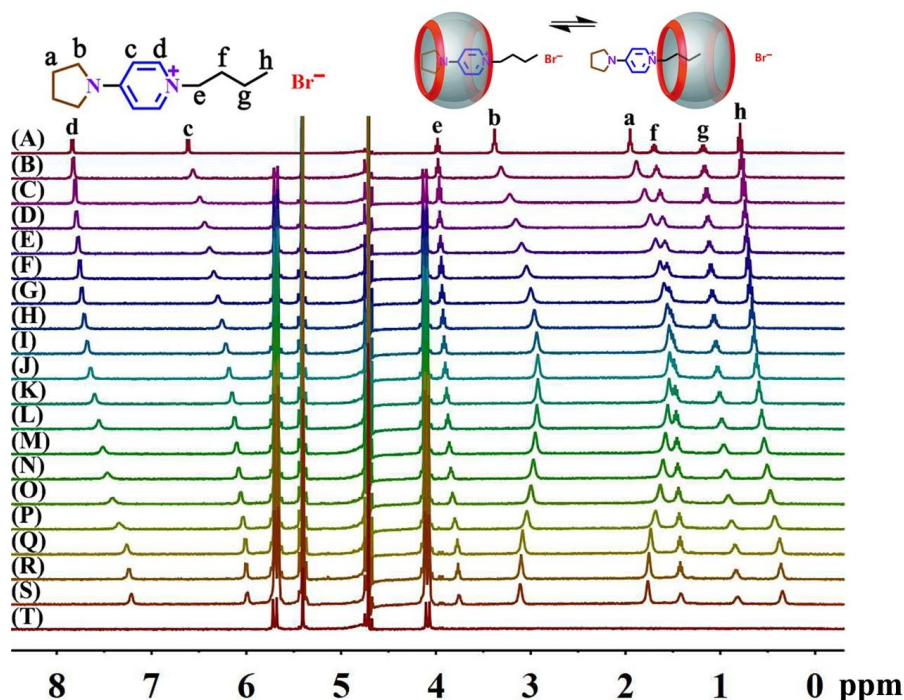

Figure 2. Interaction of g2 and Q[8] (20 °C): ^{1}H NMR spectra (400MHz, D$_2$O) of g2 (*ca.* 0.5 mM) in the absence of Q[8] (A), in the presence of 0.058 equiv. of Q[8] (B), 0.14 equiv. of Q[8] (C), 0.21 equiv. of Q[8] (D), 0.29 equiv. of Q[8] (E), 0.33 equiv. of Q[8] (F), 0.40 equiv. of Q[8] (G), 0.50 equiv. of Q[8] (H), 0.61 equiv. of Q[8] (I), 0.71 equiv. of Q[8] (J), 0.81 equiv. of Q[8] (K), 0.91 equiv. of Q[8] (L), 1.051 equiv. of Q[8] (M), 1.10 equiv. of Q[8] (N), 1.23 equiv. of Q[8] (O), 1.32 equiv. of Q[8] (P), 1.40 equiv. of Q[8] (Q), 1.46 equiv. of Q[8] (R), 1.55 equiv. of Q[8] (S), and neat Q[8] (T).

In the case of g4 and g5,

The host-guest interaction of Q[8]@g4 and Q[8]@g5 is similar, Figure 3 shows the ^{1}H NMR titration spectra of g4 in D_2O recorded in the absence of Q[8] and with increasing proportions of Q[8], and neat Q[8] in D_2O at 20 ℃. Upon the addition of Q[8], the signals of H_d and H_c of the pyridine ring, all of the alkyl chain, and H_b closest to the pyrrole N of g4 exhibited up-field shifts, while H_a of the pyrrole ring of g4 showed a slight down-field shift. At 1.15 equiv. of Q[8], H_d, H_c, H_e, H_b, H_f, and H_j of g4 experienced up-field shifts of 0.99 ppm (from 7.79 ppm to 6.80 ppm), 0.67 ppm (from 6.56 ppm to 5.89 ppm), 0.37 ppm (from 3.93 ppm to 3.56 ppm), 0.05 ppm (from 3.34 ppm to 3.29 ppm), 0.39 ppm (from 1.68 ppm to 1.29 ppm), 0.93 ppm (from 0.67 ppm to -0.26 ppm), respectively. Also H_a of g4 showed a down-field shift of 0.01 ppm (from 1.90 ppm to 1.91 ppm) compared to its position in free g4. The resonances of protons $H_{g\sim i}$ became two groups of peaks (at 0.69, 0.24 ppm) at 1.15 equiv. of Q[8], *versus* one (at 1.12 ppm) in free g4. Figure S2 displays the similar chemical shifts for all protons of g5 with increasing proportions of Q[8] to the guest at 20 ℃. These observed phenomena indicates that both in Q[8]@g4 and Q[8]@g5 systems, the pyridine ring, the alkyl chain and one part of pyrrole, namely the N-containing side, were buried inside the Q[8] cavity. The

other part of pyrrole was outside the portal. For the alkyl chain (hexyl or octyl chains) to be

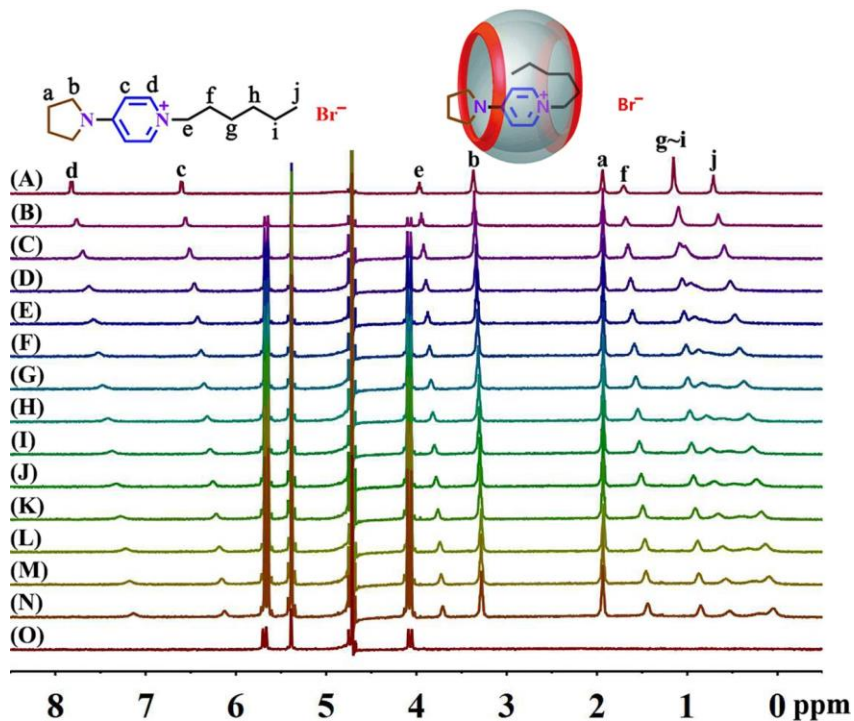buried in the cavity of Q[8], it must be present in a twisted form.

Figure 3. Interaction of g4 and Q[8] (20 °C): ^{1}H NMR spectra (400MHz, D$_2$O) of g4 (*ca.* 0.5 mM) in the

absence of Q[8] (A), in the presence of 0.073 equiv. of Q[8] (B), 0.18 equiv. of Q[8] (C), 0.33 equiv. of

Q[8] (D), 0.42 equiv. of Q[8] (E), 0.54 equiv. of Q[8] (F), 0.62 equiv. of Q[8] (G), 0.73 equiv. of Q[8] (H),

0.84 equiv. of Q[8] (I), 0.98 equiv. of Q[8] (J), 1.15 equiv. of Q[8] (K), 1.28 equiv. of Q[8] (L), 1.40 equiv.

of Q[8] (M), 1.57 equiv. of Q[8] (N), and neat Q[8] (O).

In the case of g6,

Figure 4 shows the ^{1}H NMR titration spectra of g6 in D_2O recorded in the absence of Q[8] and with increasing proportions of Q[8], and neat Q[8] in D_2O at 20 ℃. Upon addition of Q[8], H_d and H_c of the pyridine ring and all protons of the alkyl chain of g6 experienced up-field shifts, while H_b of the pyrrole ring of g6 essentially remained unchanged. The signals for H_a of g6 exhibited a down-field shift. At 1.03 equiv. of Q[8], the H_d, H_c, H_e, H_f, and H_p of g6, exhibited up-field shifts of 0.48 ppm (from 7.80 ppm to 7.32 ppm), 0.31 ppm (from 6.58 ppm to 6.27 ppm), 0.29 ppm (from 3.94 ppm to 3.65 ppm), 0.32 ppm (from 1.68 ppm to 1.36 ppm), 0.34 ppm (from 0.70 ppm to 0.36 ppm). By contrast, H_b of g6 remained essentially unchanged, while H_a of g6 underwent a down-field shift of 0.02 ppm (from 1.92 ppm to 1.94 ppm) compared to their positions in free g5. The protons $H_{g\sim o}$ became three groups of peaks (at 0.75, 0.66 and 0.46 ppm) at 1.03 equiv. of Q[8], *versus* one peak (at 1.09 ppm) in free g6. This indicates that the pyridine ring and the alkyl chain were accommodated within the cavity of Q[8] and the pyrrole ring was at its portal. The alkyl chain buried in the cavity of Q[8] was present in a twisted form, due to the long alkyl chain (dodecyl chains), and this is thought to squeeze the pyrrole ring out the cavity of Q[8] and locate it at the portal of Q[8].
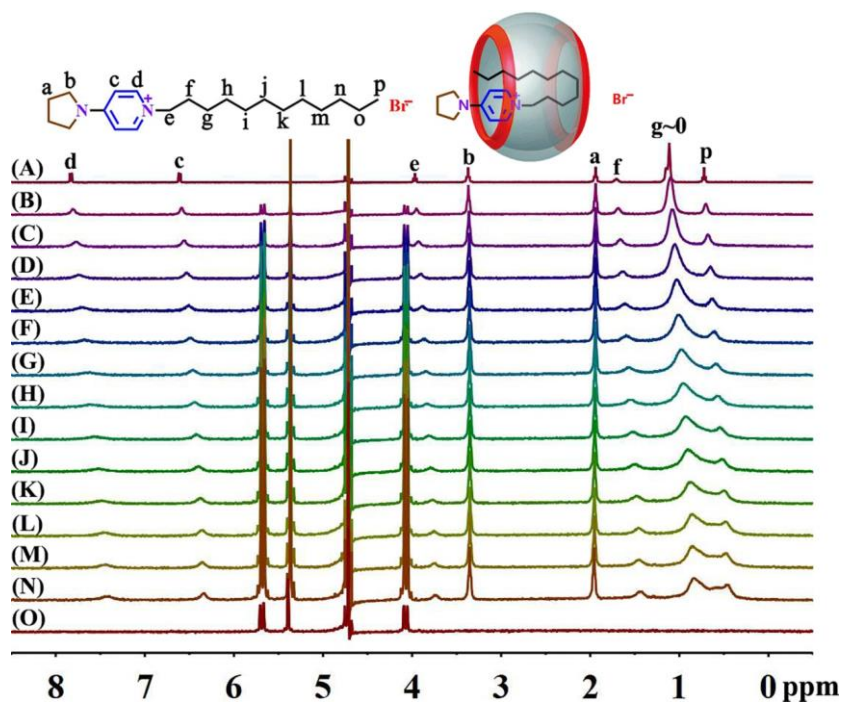
Figure 4. Interaction of g6 and Q[8] (20 ℃): ^{1}H NMR spectra (400MHz, D$_2$O) of g6 (*ca.* 0.5 mM) in the absence of Q[8] (A), in the presence of 0.08 equiv. of Q[8] (B), 0.20 equiv. of Q[8] (C), 0.33 equiv. of Q[8] (D), 0.44 equiv. of Q[8] (E), 0.51 equiv. of Q[8] (F), 0.61 equiv. of Q[8] (G), 0.71 equiv. of Q[8] (H), 0.84 equiv. of Q[8] (I), 1.03 equiv. of Q[8] (J), 1.12 equiv. of Q[8] (K), 1.22 equiv. of Q[8] (L), 1.38 equiv. of Q[8] (M), 1.48 equiv. of Q[8] (N), and neat Q[8] (O).

From the above observations, it is clear that the length of the alkyl chain plays a pivotal role in controlling the mode of the host-guest interaction.

UV spectroscopy

To further understand the binding of these 4-pyrrolidinopyridinium salts to Q[8], we also employed UV-vis spectrometry. The UV spectra were obtained using aqueous solutions containing a fixed concentration of guest g1-g6 and variable concentrations of Q[8]. As shown in Figure 5 and Figure S3-S7, the six systems show similar phenomena, and here only the interactions between Q[8] and guest g1 are described as an example. On gradually increasing the Q[8] concentration in the g1 solution, the absorption band of the guest exhibits a progressively higher absorbance due to the formation of the host-guest complex Q[8]@g1. The absorbance vs. ratio of $n(Q[8])/n(g1)$ data can be fitted to a 1:1 binding model. The pyrrolidinopyridinium part of the guest was encapsulated into the cavity of the Q[8] host, whilst the alkyl moiety remained outside. This generated a 1:1 host–guest inclusion complex. The encapsulation by Q[8] of this guest is presumably due to the favorable ion-dipole interactions between the positively charged guest and the portal oxygen atoms of Q[8] in addition to hydrophobic effects.
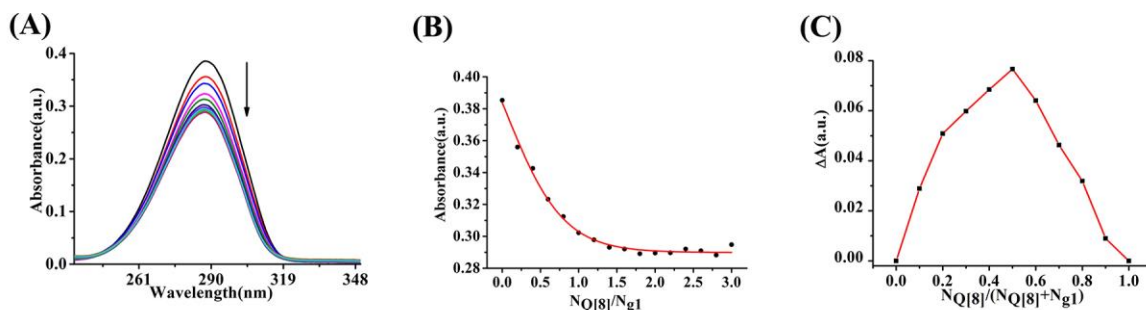
Figure 5. (Color online) (A) Electronic absorption of g1 (2×10^{-5} mol L^{-1}) upon addition of increasing amounts (0, 0.2, 0.4······2.6, 2.8, 3.0 equiv.) of Q[8]; (B) the concentrations and absorbance vs. $N_{Q[8]}/N_{g1}$ plots; (C) the corresponding ΔA–$N_{Q[8]}/(N_{Q[8]} + N_{g1})$ curves.

Mass spectrometry

The nature of the inclusion complexes between Q[8] and the 4-pyrrolidinopyridinium guests was also established by the use of MALDI-TOF mass spectra, as shown in Figure 6. Intense signals were found at 1506, 1534, 1548, 1562, 1590 and 1646, which correspond to $[(Q[8]@g1)\text{-}Br^-]^+$, $[(Q[8]@g2)\text{-}Br^-]^+$, $[(Q[8]@g3)\text{-}Br^-]^+$, $[(Q[8]@g4)\text{-}Br^-]^+$, $([(Q[8]@g5)\text{-}Br^-]^+$ and $([(Q[8]@g6)\text{-}Br^-]^+$ respectively, thereby providing support for the formation of 1:1 host-guest inclusion complexes.
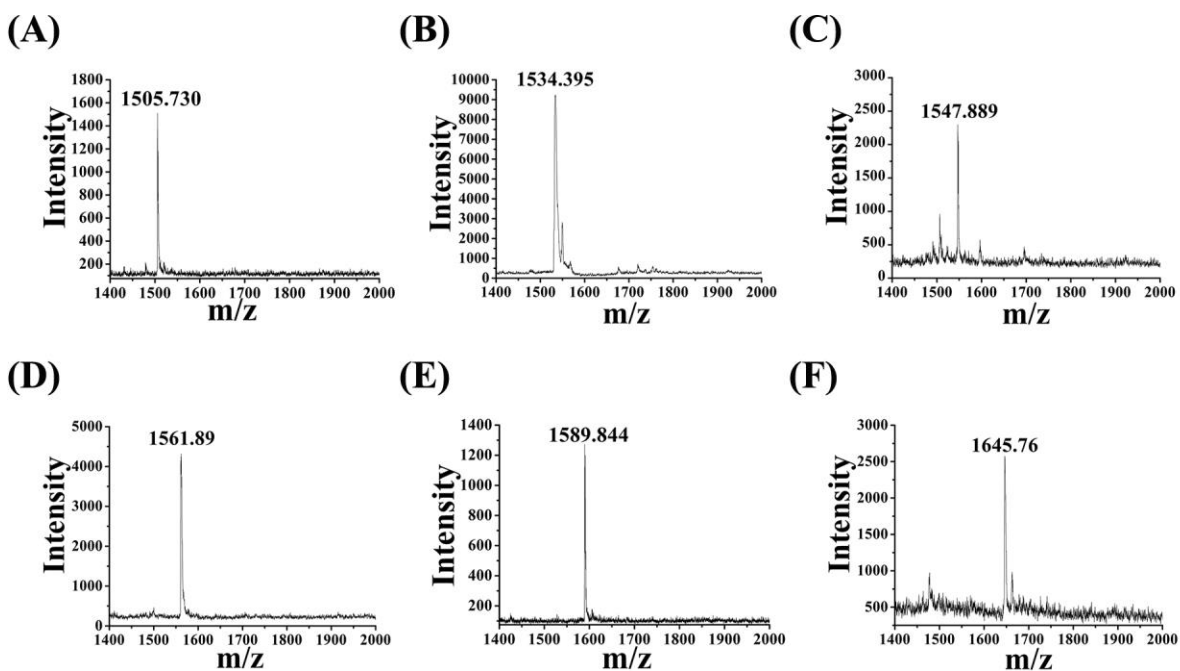
Figure 6. MALDI-TOF mass spectrometry of Q[8]@g1 (A), Q[8]@g2 (B), Q[8]@g3 (C), Q[8]@g4 (D), Q[8]@g5 (E) and Q[8]@g6 (F).

Isothermal Titration Calorimetry

A solution of each of the guests was injected into separate solutions of Q[8] at 25 °C to record the respective exothermic binding isotherms see Figure S8. The association constants K_a for g1-6 were derived from this experimental data (see table 1), with particularly high values were noted for g4-6, and negative $\Delta G°$ values ranging from -23.904 kJ/mol to -38.519 kJ/mol. All the values were consistent with the formation of stable inclusion complexes in aqueous

solution. Furthermore, the large negative values found for ΔH were consistent with a largely

enthalpy driven assembly process. The binding molar ratio in each case is 1:1.

Table 1. Data obtained from ITC experiments.

Host-Guest	$K_a/(\mathrm{M}^{-1})$	$\Delta H^{\circ}/(\mathrm{kJ \cdot mol}^{-1})$	$T\Delta S^{\circ}/(\mathrm{kJ \cdot mol}^{-1})$	$\Delta G/(\mathrm{kJ \cdot mol}^{-1})$
Q[8]-g1	1.541×10^{4}	-28.09	-4.186	-23.904
Q[8]-g2	4.714×10^{5}	-41.24	-14.081	-27.159
Q[8]-g3	8.477×10^{5}	-27.29	7.922	-35.212
Q[8]-g4	5.541×10^{6}	-35.94	2.551	-38.491
Q[8]-g5	5.597×10^{6}	-50.18	-11.661	-38.519
Q[8]-g6	3.333×10^{6}	-45.37	-8.142	-37.228

Molecular structures

There are pronounced similarities in the structure of the four molecule complexes studied for

guest g1, g2, g3, and g5. However, the length of the alkyl chain seems to be important in

directing the interaction of the guest and the Q[8]. In each host-guest structure, the asymmetric

unit contains two unique half Q[8] molecules and two unique guest molecules. (Figure 7; for

the structure of Q[8]@g1, see Figure S9 and for alternative views of the structures involving

g2, g3 and g5 see Figures S10-12 in the ESI) The centre of symmetry in each case is

responsible for generating the complete Q[8] molecules and two guest molecules in a

centrosymmetric dimer. Furthermore, in each asymmetric unit there are additionally water

molecules and charge-balancing anions. For g2 and g3 the anions present are $[CdCl_4]^{2-}$ and chloride. For g5 there is chloride and $[CdCl_3Br]^{2-}$ (where the bromide is presumably derived from the 4-pyrrolidinopyridinium bromide used in the synthesis). The additional chloride is presumably balanced by additional protons in the forms of $[H_3O]^+$ but these have not been crystallographically located. For g1 the only anion present is chloride and no Cd is present.
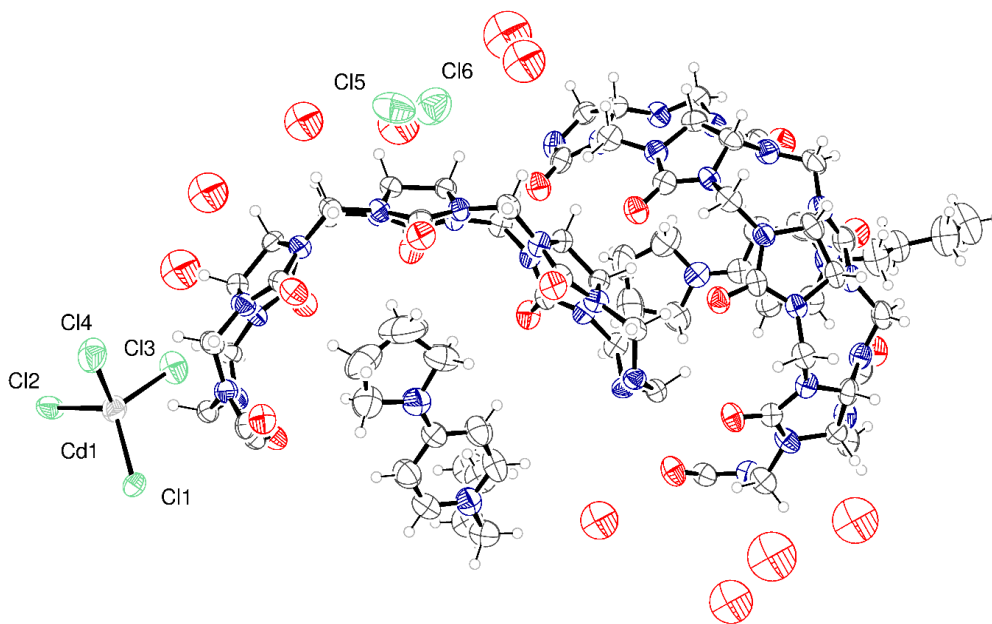

Figure 7. Asymmetric unit of Q[8]/g2 with atoms drawn as 50% probability ellipsoids.

The host-guest complexes are rather similar because each contains a centrosymmetric pair of guests and these guest are sited such that they lie at the portal of the Q[8] generating many C−H⋯O interactions. But there are important differences. For g1 and g2 the guests are encapsulated within the Q[8] such that the 5-membered ring projects into the cavity and the (short) alkyl chain is without. The orientation of the guests may be judged by the angle subtended between the 6-membered ring of the guest and the plane of the Q[8]. For g1 these

angles are 39.2 ° and 36.4 ° for the two unique Q[8] molecules. For g2 the equivalent angles are 39.0 ° and 37.9 °. (Figure 8)
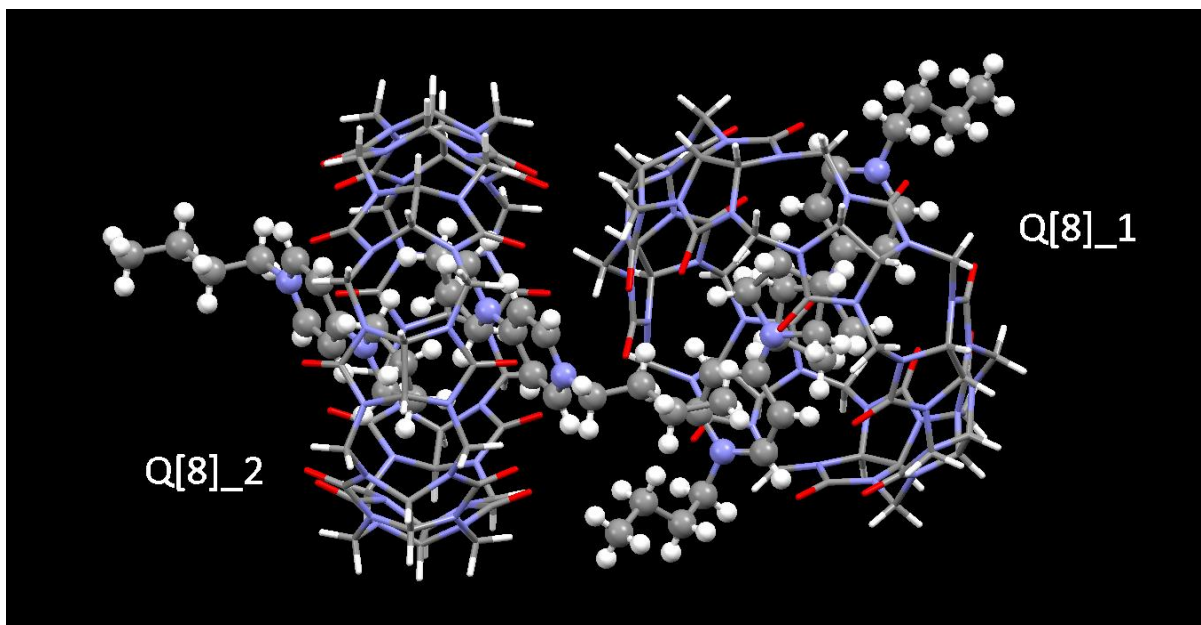

Figure 8. Docking of g2 inside the Q[8] (alkyl chain within cavity).

For g3 there are two unique Q[8] rings and these contains guests with differing orientation (Figure 9). For one Q[8] it is the 5-membered ring of the (two) guests that project into the ring (alkyl chain without). But for the second Q[8] the alkyl chains of the g3 guest molecules project into the cavity and the 5-membered rings are without. The angles between host/guest between the 6-ring and Q[8] are 37.2 ° (5-ring within) and 26.2 ° (5-ring without). (Figure 10) For g5 the alkyl chain of the guest is poorly resolved crystallographically, but it is clear that it is this end of the guest molecule that is within the cavity and not the 5-membered ring. For g5 the angle of approach of the molecules are 40.5 ° and 47.8 °.
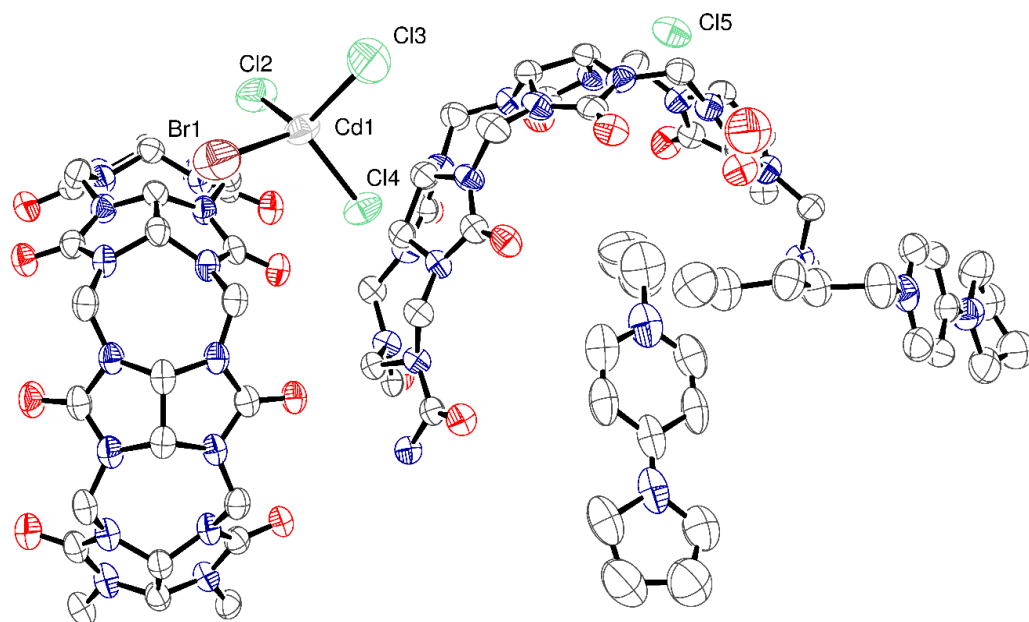
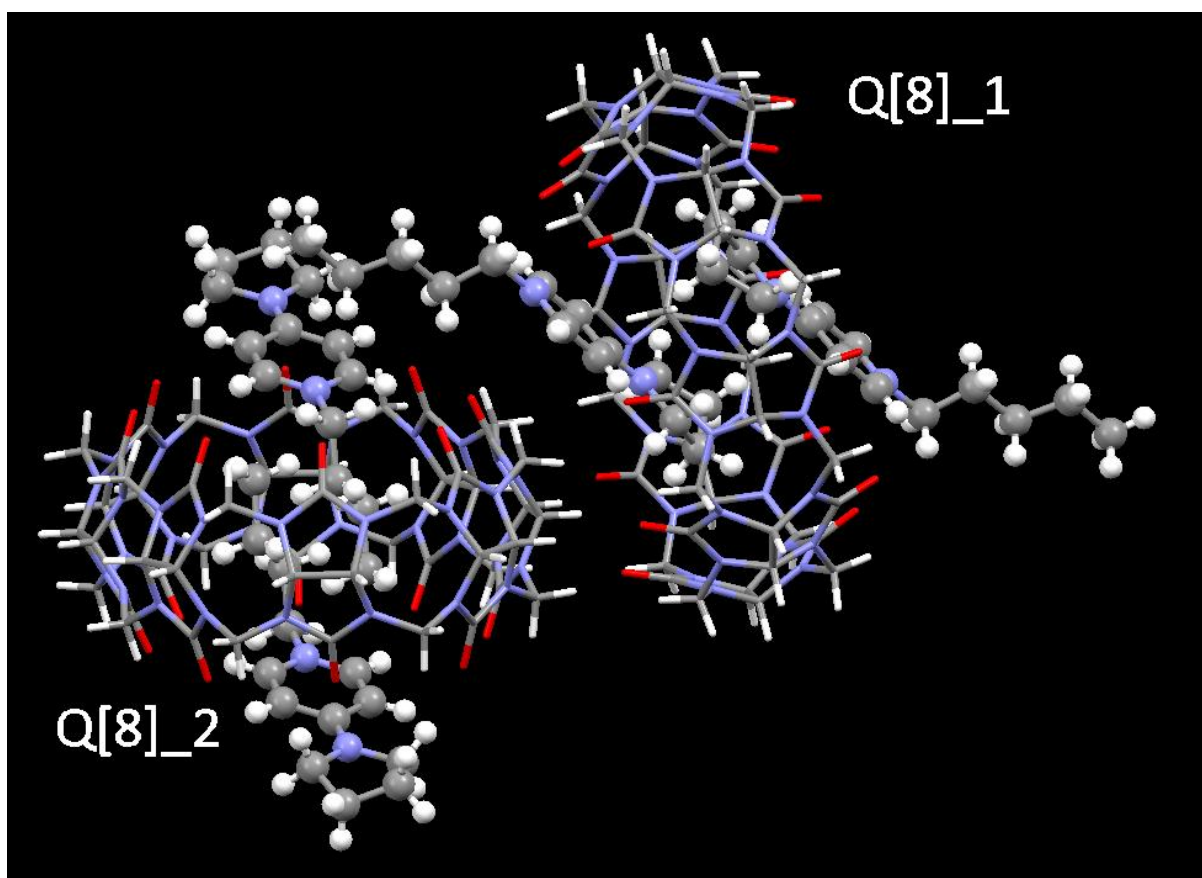**Figure 9**. Asymmetric unit of Q[8]/g3 with atoms drawn as 50% probability ellipsoids.

Figure 10. Docking of g3 inside the Q[8]. For Q[8]_1 the alkyl chain lies outside of the cavity. For Q[8]_2 the alkyl chain is within the cavity.

Experimental Section

To analyze the host–guest complexation between Q[8] and g1/g2/g3/g4/g5/g6, 2.0–2.5×10^{-3} mmol solutions of Q[8] in 0.5–0.7 mL D_2O with Q[8]: g1/g2/g3/g4/g5/g6 ratios ranging between 0 and 2 were prepared. All ^{1}H NMR spectra, including those for the titration experiments, were recorded at 298.15 K on a JEOL JNM-ECZ400S 400 MHz NMR spectrometer (JEOL) in D_2O. D_2O was used as a field-frequency lock, and the observed chemical shifts are reported in parts per million (ppm).

All UV-visible spectra were recorded from samples in 1 cm quartz cells on an Agilent 8453 spectrophotometer, equipped with a thermostat bath (Hewlett Packard, California, USA). The host and guests were dissolved in distilled water. UV-visible spectra were obtained at 25 °C at a concentration of 2.00×10^{-5} mol·L^{-1} gi (i=1,2,3,4,5,6) and different Q[8] concentrations for the Q[8]@gi (i=1,2,3,4,5,6) system. MALDI-TOF mass spectrometry was recorded on a Bruker BIFLEX III ultra-high resolution Fourier transform ion cyclotron resonance (FT-ICR) mass spectrometer with α-cyano-4-hydroxycinnamic acid as matrix. 4-pyrrolidinopyridine was purchased from Aladdin Industrial Corporation, and Q[8] was prepared and purified according to previously published methods[11]. Given acid (HCl) was employed during the synthesis of Q[8] the pH value of the solvent is *ca.* 5.4. All other reagents were of analytical grade and were used as received. Double-distilled water was used for all experiments. ^{1}H and ^{13}C NMR spectra of the guests g1 – g6 are presented in Figures S13-S18 in the ESI.

Synthesis of guest g1

4-pyrrolidinopyridine (296 mg, 0.002 mol) and bromoethane (1.308 g, 0.012 mol) were dissolved in acetonitrile (40 ml). The solution was stirred under an inert nitrogen atmosphere and heated to 80 °C and refluxed for 12 h. The resulting solution was filtered and then the yellow precipitate was washed with diethyl ether and then dried in vacuum to give g1 (437 mg, 85%). ^{1}H NMR (D_2O, 400 MHz) δ 7.78 (d, J = 7.6 Hz, 2H), 6.54 (d, J = 7.5 Hz, 2H), 3.94 (q, J = 7.3 Hz, 2H), 3.30 (m, J = 8.0 Hz, 4H), 1.90 – 1.84 (m, 4H), 1.25 (t, J = 7.3 Hz, 3H). Anal. Calcd. for $C_{11}H_{17}N_2Br$: C, 51.37; H, 6.66; N, 10.89; found C, 51.29; H, 6.71; N, 10.92.

Synthesis of guest g2

The same synthesis method as for g1 was employed, but using 4-pyrrolidinopyridine (296 mg, 0.002 mol) and bromobutane (1.644 g, 0.012mol) to give g2 (496 mg, 87%). ^{1}H NMR (D_2O, 400 MHz) δ 7.79 (d, J = 7.6 Hz, 2H), 6.57 (d, J = 7.5 Hz, 2H), 3.94 (t, J = 7.1 Hz, 2H), 3.34 (t, J = 6.7 Hz, 4H), 1.93 – 1.88 (m, 4H), 1.66 (m, J = 14.8 Hz, 2H), 1.14 (m, J = 14.8 Hz, 2H), 0.75 (t, J = 7.4 Hz, 3H). Anal. Calcd. for $C_{13}H_{21}N_2Br$: C, 54.74 ; H, 7.42; N, 9.82; found C, 54.82; H, 7.47; N, 9.75.

Synthesis of guest g3

The same synthesis method as for g1 was employed, but using 4-pyrrolidinopyridine (296 mg, 0.002 mol) and bromopentane (1.813 g, 0.012mol) to give g3 (508 mg, 85%). ^{1}H NMR (D_2O, 400 MHz) δ 7.75 (d, J = 7.6 Hz, 2H), 6.53 (d, J = 7.6 Hz, 2H), 3.90 (t, J = 7.1 Hz, 2H), 3.30 (t, J = 6.8 Hz, 4H), 1.89 – 1.84 (m, 4H), 1.64 (m, J = 14.5 Hz, 2H),

1.18 – 0.99 (m, 4H), 0.66 (t, J = 8.8Hz, 3H). Anal. Calcd. for $C_{14}H_{23}N_2Br$: C, 56.19; H, 7.75; N, 9.36; found C, 56.14; H, 7.81; N, 9.39.

Synthesis of guest g4

The same synthesis method as for g1 was employed, but using 4-pyrrolidinopyridine (296 mg, 0.002 mol) and bromohexane (1.981 g, 0.012mol) to give g4 (551 mg, 88%). ^{1}H NMR (D$_2$O, 400 MHz) δ 7.79 (d, J = 7.0 Hz, 2H), 6.57 (d, J = 7.1 Hz, 2H), 3.94 (q, J = 7.0 Hz, 2H), 3.35 (d, J = 6.1 Hz, 4H), 1.91 (m, 4H), 1.68 (m, J = 6.6 Hz, 2H), 1.12 (m, 6H), 0.69 (t, J = 6.4 Hz, 3H). Anal. Calcd. for $C_{15}H_{25}N_2Br$: C, 57.51; H, 8.04; N, 8.94; found C, 57.48; H, 8.11; N, 8.99.

Synthesis of guest g5

The same synthesis method as for g1 was employed, but using 4-pyrrolidinopyridine (296 mg, 0.002 mol) and 1-bromooctane (2.318 g, 0.012mol) to give g5 (593 mg, 87%). ^{1}H NMR (D$_2$O, 400 MHz) δ 7.79 (d, J = 7.0 Hz, 2H), 6.57 (d, J = 7.1 Hz, 2H), 3.94 (t, J = 7.0 Hz, 2H), 3.35 (d, J = 6.1 Hz, 4H), 1.91 (m, 4H), 1.68 (m, J = 6.6 Hz, 2H), 1.12 (m, 10H), 0.69 (t, J = 6.4 Hz, 3H). Anal. Calcd. for $C_{17}H_{29}N_2Br$: C, 59.82; H, 8.56; N, 8.21; found C, 59.89; H, 8.59; N, 8.14.

Synthesis of guest g6

The same synthesis method as for g1 was employed, but using 4-pyrrolidinopyridine (296 mg, 0.002 mol) and 1-bromododecane (2.991 g, 0.012mol) to give g6 (659 mg, 83%). ^{1}H NMR (D$_2$O, 400 MHz) δ 7.81 (d, J = 7.3 Hz, 2H), 6.59 (d, J = 7.4 Hz, 2H), 3.95 (t, J = 6.9 Hz, 2H), 3.35 (t, J = 6.4 Hz, 4H), 1.93 (m, J = 6.7 Hz, 4H), 1.70 (d, J = 6.9 Hz, 2H), 1.11 (m, 18H), 0.70 (t, J = 6.7 Hz, 3H). Anal. Calcd. for $C_{21}H_{37}N_2Br$: C, 63.46; H, 9.38; N, 7.05; found C, 63.40; H, 9.42; N, 7.10.

Synthesis of the inclusion complex Q[8]·g1

Q[8] (7.54 mg, 0.005 mmol) and g1 (12.86 mg, 0.050 mmol) were dissolved in HCl (4 mL, 6mol/L). The mixture was then heated until complete dissolution. Slow evaporation of the volatiles from the solution over a period of about two weeks provided colorless crystals.

Synthesis of the inclusion complex Q[8]·g2

Q[8] (7.54mg, 0.005 mmol), g2 (14.26 mg, 0.050 mmol) and $CdCl_2·4H_2O$ (11.8 mg, 0.051 mmol) were dissolved in HCl (4 mL, 6mol/L). The mixture was heated until complete dissolution. Slow evaporation of the volatiles from the solution over a period of about two weeks provided colorless crystals.

Synthesis of the inclusion complex Q[8] g3

Q[8] (7.54 mg, 0.005 mmol), g3 (14.96mg, 0.050 mmol) and $CdCl_2·2H_2O$ (11.8 mg 0.051 mmol) were dissolved in HCl (4 mL, 6mol/L). The mixture was heated until complete dissolution. Slow evaporation of the volatiles from the solution over a period of about two weeks provided colorless crystals.

Synthesis of the inclusion complex Q[8] g5

Q[8] (7.54 mg, 0.005 mmol), g5 (17.07 mg, 0.050 mmol) and $CdCl_2·2H_2O$ (11.8 mg 0.051 mmol) were dissolved in HCl (4 mL, 6mol/L). The mixture was heated until complete dissolution. Slow evaporation of the volatiles from the solution over a period of about two weeks provided colorless crystals.

ITC measurements

Microcalorimetric experiments were performed using an isothermal titration calorimeter Nano ITC (TA, USA). The experiments of g1 with Q[8] and g2 with Q[8] consisted of 40 consecutive injections (6 µL) of a guest solution into the microcalorimetric reaction cell (1.3 mL) charged with a solution of Q[8]. The experiments of g3 with Q[8] and g4 with Q[8] consisted of 30 consecutive injections (4 µL) of a guest solution into the microcalorimetric reaction cell (1.3 mL) charged with a solution of Q[8].The experiments of g5 with Q[8] and g6 with Q[8] consisted of 25 consecutive injections (10 µL) of a guest solution into the microcalorimetric reaction cell (1 mL) charged with a solution of Q[8] at 25 °C. The heat of reaction was corrected for the heat of dilution of the guest solution determined in separate experiments. All solutions were degassed prior to titration experiment by sonication. Computer simulations (curve fitting) were performed using the Nano ITC analyze software.

Crystal structure determinations

Diffraction data for the inclusion complexes Q[8]·g2 and Q[8]·g3 were collected at 293 K with a Bruker SMART Apex-II CCD diffractometer using graphite-monochromated Mo-Kα radiation (λ=0.71073 Å). Structural solution and full-matrix least-squares refinement based on F^2 were performed with the SHELXS-97 and SHELXL-2014 program packages, respectively. [12, 13] All non-hydrogen atoms were refined with anisotropic displacement parameters. The carbon-bound hydrogen atoms were introduced at calculated positions. All hydrogen atoms were treated as riding atoms with an isotropic displacement parameter equal to 1.2 times that of the parent atom. For each inclusion complex the unit cell includes a large amount of isolated water molecules. We employed PLATON/SQUEEZE [14] to calculate the diffraction contribution of the solvent molecules and, thereby, to produce a set of solvent-free

diffraction intensities. In each structure there is one additional chloride ion present beyond that required to balance the charge of the 4- pyrrolidinopyridinium. Crystals are grown from acidic solution; presumably, some H^+ is included in the form of H_3O^+ to balance the charge.

Conclusions

In summary, we have investigated the binding interactions of Q[8] with a series of 4-pyrrolidinopyridinium guests, bearing aliphatic substituents at the pyridinium nitrogen, using ^{1}H NMR and UV spectroscopy, mass spectrometry, Isothermal Titration Calorimetry and X-ray crystallography. In aqueous solution (D_2O), the alkyl chain at the pyridinium nitrogen can either reside in the Q[8] cavity along with the rest of the guest (as observed for g4, g5 and g6), can be out found outside the Q[8] with the rest of the guest inside (as seen for g1) or two species can exist in equilibrium for which either the chain or the rest of the guest is encapsulated by the Q[8]. In the solid-state, the structures are somewhat different. In the case of Q[8]@g2, two Q[8] molecules are filled with a centrosymmetric pair of guest molecules, with the cyclic amine encapsulated with the molecule enters at a rather shallow angle. Interestingly for Q[8]@g3, the two Q[8] molecules behave in different ways. In particular, for one Q[8], the cyclic amine of the guest enters the ring at a rather shallow angle, but for the other Q[8] it is the alkyl chain of the guest that enters the ring with the four carbon atoms of the alkyl chain almost perpendicular to the cavity opening and almost completely encapsulated by the Q[8].

Table 1. Crystallographic data

Compound	*Q[8]/g1*	*Q[8]/g2*	*Q[8]/g3$^+$*	*Q[8]/g5*
Formula	$C_{48}H_{48}N_{32}O_{16}$, $2(C_{11}H_{17}N_2)$, 2Cl, $18H_2O$	$C_{48}H_{48}N_{32}O_{16}$, $2(C_{13}H_{21}N_2)$, $CdCl_4$, Cl, $13H_2O$	$C_{48}H_{48}N_{32}O_{16}$, $2C_{14}H_{23}N_2$, Br Cd Cl_3, Cl, $6H_2O$	$C_{48}H_{48}N_{32}O_{16}$, $C_{11}H_{12}N_2$, Cd Cl_4, 2Cl, $15H_2O$
Formula weight	1882.61	2189.46	2117.98	2110.65
Crystal system	Triclinic	Triclinic	Triclinic	Triclinic
Space group	P-1	P-1	P-1	P-1
Unit cell dimensions				
a (Å)	17.419(5)	17.3794(9)	16.5084(6)	17.6475(4)
b (Å)	17.601(5)	18.2084(9)	16.7146(8)	17.9279(4)
c (Å)	17.791(5)	18.4713(9)	19.6872(6)	18.1492(4)
α (Å)	88.312(7)	88.097(2)	84.261(3)	64.6200(10)
β (Å)	89.035(8)	75.007(2)	76.978(3)	82.5400(10)
γ (Å)	66.890(7)	65.953(2)	69.172(4)	89.4350(10)
V (Å^3)	5014(2)	5138.9(5)	4945.6(4)	5137.3(2)
Z	2	2	2	2
Temperature (K)	293(2)	293(2)	293(2)	293(2)
Wavelength (Å)	0.71073	0.71073	0.71073	1.54178
Calculated density (Mg m^{-3})	1.247	1.415	1.422	1.364
Absorption coefficient (mm^{-1})	0.147	0.429	0.812	3.851
Transmission factors (min/max)	0.6515 and 0.7457	0.889 and 0.927	0.829 and 0.854	0.5216 and 0.7524
Crystal size (mm^3)	0.260 x 0.240 x 0.230	0.280 x 0.250 x 0.180	0.240 x 0.230 x 0.200	0.240 x 0.225 x 0.180
θ (max) (°)	25.027	25.219	25.121	63.751
Reflections measured	58517	56325	27261	44875
Unique reflections	17660	18292	17155	16355
R_{int}	0.1087	0.0604	0.0274	0.0347
Reflections with $F^2 > 2\sigma(F^2)$	17660	11364	13261	16355
Number of parameters	1139	1223	1204	1052
$R_1 [F^2 > 2\sigma(F^2)]$	0.1263	0.1014	0.0835	0.1112

wR$_2$ (all data)	0.3896	0.3493	0.2468	0.3909
GOOF, S	1.149	1.253	1.036	1.783
Largest difference peak and hole (e Å^{-3})	0.983 and -1.185	2.114 and -0.773	3.575 and -1.478	1.958 and -2.049

CCDC 1849748=1849749 and 1872252-1872253 contain the supplementary crystallographic data for this paper and available free of charge from ccdc.cam.ac.uk

References

[1] For a recent review, see (a) Barrow, S. J.; Kasera, S.; Rowland, M. J.; del Barrio, J.; Scherman, O. A. *Chem. Rev*. 2015, **115**, 12320-12406. (b) Gao, R. H.; Chen, L. X.; Chen, K.; Tao, Z.; Xiao, X. *Coord. Chem. Rev.* 2017, **348**, 1-24. (c) Assaf, K. I.; Nau, W. M.; *Chem. Soc. Rev*., 2015,**44**, 394-418 .(d) Zhang, M.; Yan, X.; Huang, F.; Niu, Z.; Gibson, H. W. *Acc. Chem.*

Res. 2014, **47**, 1995-2005. (e) Lyle, I. *Acc. Chem. Res*., 2014, **47**, 2052-2062. (f) Yu, G.; Jie, K.; Huang, F. *Chem. Rev.* 2015, **115**, 7240-7303. (g) Wei, P.; Yan, X.; Huang, F. *Chem. Soc. Rev.* 2015, **44**, 815-832. (h) Liu, J.; Lan, Y.; Yu, Z.; Tan, C. S. Y.; Parker, R. M.; Abell, C.; Scherman, O. A. *Acc. Chem. Res.*, 2017, **50**, 208-217. (i) Kaifer, A. E., *Acc. Chem. Res.* 2014, **47**, 2160-2167.

[2] (a) Lagona, J.; Mukhopadhyay P.; Chakrabarti S. and Isaacs L. *Angew. Chem. Int. Ed.* 2005, **44**, 4844. (b) Yang, B.; Yu, S. B.; Wang, H.; Zhang, D. W.; Li, Z. T. *Chem. Asian. J,* 2018, **13**, 1312-1317. (c) Aryal, G. H.; Hunter, K.W. and Huang, L. M. *Org. Biomol. Chem.* 2018, **16**, 7425-7429. (d) Gao, Z. Z.; Kan, J. L.; Tao, Z.; Bian, B.; Xiao, X. *New J. Chem.,* 2018, **42**, 15420-15426. (e) Ding, Y.; Yang, B.; Liu, H.; Liu, Z.; Zhang, X.; Liu, Q. *Sensor Actuat B: Chem.*, 2018, **259**, 775-783. (f) Wang, X.X.; Chen, K.; Shen, F. F.; Hua, Z. Y.; Qiu, S. C.; Zhang, Y. Q.; Cong, H.; Liu, Q. Y.; Tao, Z.; Xiao, X. *Chem. Eur. J.,* 2017, **23(67)**, 16953-16956; (g) Bai, D.; Zhou, Y.; Lu, J. H.; Liu, Q. Y.; Chen, Q.; Tao, Z. Xiao, X. *Chin. J. Org. Chem.* 2018, **38**, 1477-1483.

 [3] (a) Barrow, S. J.; Kasera, S.; Rowland, M. J.; Barrio, J. Del.; Scherman, O. A. *Chem. Rev.* 2015, **115**, 12320-12406. (b) Assaf, K. I.; Nau, W. M. Chem. Soc. Rev. 2015, **44**, 394-418. (c) Chen, L. X.; Kan, J. L.; Cong, H.; Prior, T. J.; Tao, Z.; Xiao, X.; Redshaw, C. *Molecules.* 2017, **22(7)**, 1147-1154. (d) Ji, L.; Yang, L.; Yu, Z.Y.; Tan, C. S. Y.; Parker, R. M.; Abell, C.;

Scherman, O. A. *Accounts. Chem. Res.* 2017, **50(2)**, 208-217. (e) Xiao, X.; Sun, J. S.; Jiang, J. Z. *Chem. Eur. J.* 2013, **19**, 16891-16896.

[4] (a) Gao, Z.; Bai, D.; Chen, I.; Tao, Z.; Xiao, X.; Prior, T. J.; Redshaw, C. *RSC Adv*. 2017. **7**, 461-467. (b) Bai, D.; Gao, Z.; Tao, Z.; Xiao, X.; Prior, T. J.; Wei, G.; Liu Q.; Redshaw, C. *New J. Chem*. 2018, **42**, 11085-11092. (c) Meng, T.-H.; Zhou, Y.; Gao, Z.-Z.; Liu, Q.-Y., Tao, Z.; Xiao, X. *J. Incl. Phenom. Macro. Chem.*, 2018, **90**, 357-363

 [5] Hou, H.; Gao, Z.; Bai, D.; Tao, Z.; Prior, T. J.; Redshaw, C.; Xiao, X. *Supramol. Chem.* 2017, **29**, 680-685.

[6] (a) Yamanaka, M.; Yoshida, U.; Sato, M.; Shigeta, T.; Yoshida, K.; Furuta, T.; Kawabata, T. J. *Org. Chem.* 2015, **80**, 3075–3082. (b) Sammaki, T.; Hurley, T. B. *J. Am. Chem. Soc*. 1996, **118**, 8967– 8968. (c) Nguyen, H. V.; Butler, D. C. D.; Richards, C. J. *Org. Lett*. 2006, **8**, 769–772.

[7] (a) Zanotti, G.; Scapin, G.; Spadon, P.; Veerkamp, J. H. and Sacchettini, J. C. *J. Biol. Chem.* 1992, **267**, 18541. (b) Han, G. W.; Lee, J. Y.; Song, H. K.; Chang, C.; Min, K.; Moon, J.; Shin, D. H.; Kopka, M. L.; Sawaya, M. R. and Yuan, H. S. *J. Mol. Biol.* 2001, **308**, 263. (c) Scarso, A.; Trembleau, L. and Rebek, J.; Jr. *Angew. Chem.* 2003, **115**, 5657. (d) Gao, Y.; Wu, K.; Li, H.; Chen, W.; Fu, M.; Zhu, K.; Yue, X.; Liu, Q. *Sensor Actuat B:*

Chem., 2018, **273**, 1635-1639. (e) Ko, Y. H.; Kim, H.; Kim, Y.; Kim, K. *Angew. Chem.* 2008, **120**, 4174.

[8] Trembleau, L.; Rebek, J., Jr. Science2003, 301, 1219−1220.

[9] (a) Ko, Y. H.; Kim, H.; Kim, Y.; Kim, K.Angew. Chem., Int. Ed. 2008, 47, 4106−4109. (b) Baek, K.; Kim, Y.; Kim, H.; Yoon, M.; Hwang, I.; Ko, Y. H.; Kim, K.Chem. Commun.2010, 4091−4093. (c) Ko, Y. H.; Kim, Y.; Kim, H.; Kim, K. Chem.‐Asian J.2011, 6(2), 652−657.

[10] Xiao, X.; Wang, Q.; Yu, Y.-H.; Xiao, Z.-Y.; Tao, Z.; Xue, S.-F.; Zhu, Q.-J.; Liu, J.-X.; Liu, X.-H., *Eur. J. Org. Chem.*, 2011, 2366–2371.

[11] (a) Day, A.; Arnold, A. P.; Blanch, R. J.; Snushall, B. *J. Org. Chem.*, 2001, **66**, 8094-8100. (b) Kim, J.; Jung, I. S.; Kim, S, Y. Lee, E.; Kang, J. K.; Sakamoto, S.; Yamaguchi, K.; Kim, K. *J. Am. Chem. Soc.,* 2000, **122**, 540-541.

[12] Sheldrick, G, M. *Acta Cryst*. 2008, **A64**, 112-122.

[13] Sheldrick, G. M. *Acta Cryst*. 2015. C**71**, 3-8.

[14] Spek, A. L. *Acta Cryst*. 2009, D**65**, 148-155.